to Jahn–Teller distortion. A distortion of the axial bonds along the Berry psuedorotation coordinate would lower the symmetry to C_{2v} and generate the energy diagram shown in Figure 2, column e, for the iron 3d orbitals. The result is a net stabilization of the system and the distortion is therefore anticipated. Under such conditions, the absorption spectrum analysis may be even further complicated. We observe that the $FeCl_3(PR_3)_2$ (R = Ph, Me) structures *in the solid state* (see above) do not show a strong deviation of the P–Fe–P moiety from linearity [P(1)–Fe–P(2) = 172.4 (1)° for R = Ph, 176.3 (2)° for R = Me]. In fact, the structure of the PPh_3 compound, which is in a pure $S = {}^5/_2$ spin state and therefore not expected to give rise to Jahn–Teller distortion, appears more distorted than the structure of the PMe_3 compound. On the other hand, the Cl–Fe–Cl angles deviate more from the expected 120° value in the PMe_3 compound [115.1 (2) and twice 122.46 (9)° vs 122.6 (2), 118.3 (1), and 119.1 (2)° for the PPh_3 compound]. These small deviations are probably due to packing effects.

Acknowledgment. We are grateful to the University of Maryland, College Park (UMCP), MD, Chemistry Department, the UMCP General Research Board, the Camille and Henry Dreyfus Foundation (through a Distinguished New Faculty Award to R.P.), and the donors of the Petroleum Research Fund, administered by the American Chemical Society, for support. The X-ray diffractometer and MicroVax computer system were purchased in part with NSF funds (Grant CHE-84-02155). We thank Dr. L. Bennett and L. J. Swartzendruber for the SQUID solid-state variable-temperature magnetic studies on $FeCl_3(PMe_3)_2$ at the National Institute of Standards and Technology, Gaithersburg, MD. We also thank Profs. N. S. Dalal, B. M. Hoffman, and E. I. Solomon and one of the reviewers for helpful comments and Prof. H. Ammon for technical assistance with the X-ray diffractometer.

Supplementary Material Available: Full tables of crystal data, bond lengths, bond angles, and anisotropic displacement parameters for $FeCl_3(PPh_3)_2$, $FeCl_3(PMe_3)_2$, and $[PHPh_3][FeCl_4]$ and a table of positional parameters for $[PHPh_3][FeCl_4]$ (21 pages); listings of calculated and observed structure factors for $FeCl_3(PPh_3)_2$, $FeCl_3(PMe_3)_2$, and $[PHPh_3][FeCl_4]$ (73 pages). Ordering information is given on any current masthead page.

Contribution from the Department of Chemistry, University of Helsinki, Et. Hesperiankatu 4, 00100 Helsinki, Finland, and Department of Macromolecular Chemistry, Faculty of Science, Osaka University, Toyonaka, Osaka 560, Japan

REX Calculations. 12. Iteration Parameters for the 5f-Element Organometallics of Thorium–Neptunium. Geometries of ThO_2 and UO_2^{2+} Revisited

Pekka Pyykkö,*,† Liisa J. Laakkonen,† and Kazuyuki Tatsumi*,‡,§

Received July 29, 1988

Iterative relativistic extended Hückel (REX) energy parameters giving realistic metal orbital populations for organometallic compounds are presented for the early actinoids, An = Th–Np. The energy levels for $An(C_8H_8)_2$ are also reasonable. A transition from $5f\delta$ toward $5f_{5/2}$ bonding is noticed in the actinocene series. The problem "Why is uranyl linear while the isoelectronic ThO_2 is bent?" is revisited within the REX model.

1. Introduction

The object of the present work is to see whether a realistic description of the electronic structure of the organometallic compounds of the early actinoids (Th–Np) is possible at the crudest semiempirical level, viz. the extended Hückel (EH) one. Our relativistic extended Hückel method (REX) contains the radial and energetic relativistic effects, including spin–orbit splitting, but its earliest applications on actinoid systems[1] were noniterative and led to an exaggerated ionicity.

One can outline three philosophies for EH calculations.[2] (1) "Organic" with the traditional Hoffmann parameters, no iterations, and no Madelung corrections; (2) "organometallic" with the traditional ligand parameters and iterations for the metal atoms only, without Madelung corrections; (3) "inorganic" in which all atoms are iterated, with the Madelung corrections. Simulating the Hartree-Fock method, this method gives decent MOs and orbital energies but no well-defined total energy. For recent reviews, see ref 2 and 3. In cases 1 and 2, a reasonable description of all properties (atomic populations of the MOs, relative orbital energies, and total energies) is attempted.

Charge iterations were added to REX following method 3 in ref 4. We now consider philosophy 2 for REX using the metal characters and orbital energies from earlier scattered wave,[5–7] relativistic HFS,[8] and pseudopotential HF[9] data on the actinocenes, $An(COT)_2$ (COT = C_8H_8), or cyclopentadienyls, $An(cp)_4$ (cp = C_5H_5), as reference points.

We also report quasirelativistic (QR), one-component averages of the present radial and energetic parameters. They can be used in traditional EH programs and contain the other relativistic effects, apart from spin–orbit splittings. Applications have already been published.[10,11]

Finally we return to the issue "Why is uranyl linear and the isoelectronic ThO_2 bent?"[1,4,12–14] An aspect not fully considered before is the influence of the bond length.

†University of Helsinki.
‡Work performed at the University of Helsinki under a scholarship from the Neste Oy Foundation.
§Osaka University.

(1) Pyykkö, P.; Lohr, L. L., Jr. *Inorg. Chem.* **1981**, *20*, 1950.
(2) Pyykkö, P. In *Methods in Computational Chemistry*; Wilson, S., Ed.; Plenum Press: London and New York, 1988; Vol. 2. This review also contains a diskette with the ITEREX program for an IBM PC.
(3) Albright, T. A.; Burdett, J. K.; Whangbo, M.-H. *Orbital Interactions in Chemistry*; Wiley: New York, 1985.
(4) Larsson, S.; Pyykkö, P. *Chem. Phys.* **1986**, *101*, 355.
(5) Rösch, N.; Streitwieser, A., Jr. *J. Am. Chem. Soc.* **1983**, *105*, 7237.
(6) Rösch, N. *Inorg. Chim. Acta* **1984**, *94*, 297.
(7) Bursten, B. E.; Casarin, M.; di Bella, S.; Fang, A.; Fragalà, I. L. *Inorg. Chem.* **1985**, *24*, 2169.
(8) (a) Boerrigter, P. M. Spectroscopy and Bonding of Heavy Element Compounds. Thesis, Vrije Universiteit: Amsterdam, 1987. (b) Boerrigter, P. M.; Baerends, E. J.; Snijders, J. G. *Chem. Phys.* **1988**, *122*, 357.
(9) Chang, A. H. H.; Pitzer, R. M. Submitted for publication.
(10) Tatsumi, K.; Nakamura, A. *Organometallics* **1987**, *6*, 427.
(11) Tatsumi, K.; Nakamura, A. *J. Am. Chem. Soc.* **1987**, *109*, 3195.
(12) Tatsumi, K.; Hoffmann, R. *Inorg. Chem.* **1980**, *19*, 2656.
(13) Wadt, W. R. *J. Am. Chem. Soc.* **1981**, *103*, 6053.
(14) Pyykkö, P.; Laaksonen, L. *J. Phys. Chem.* **1984**, *88*, 4892.

0020-1669/89/1328-1801$01.50/0

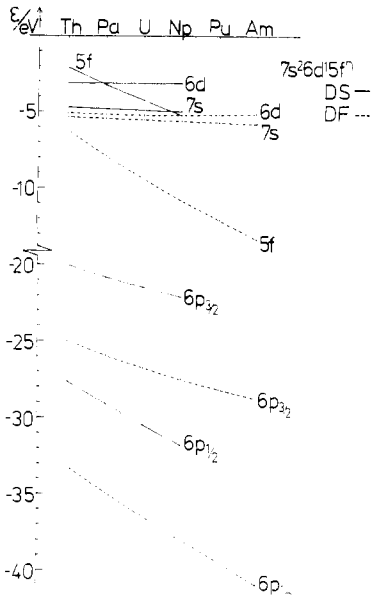

Figure 1. Orbital energies (eV) for $7s^26d^15f^n$ configurations of actinoid atoms: full curves, Dirac–Slater (DS) (present work); dashed curves, Dirac–Fock (DF) (Desclaux[16] and Pyykkö and Laaksonen[14]). The lower j value of $l - {}^1/_2$ is given for 6d and 5f orbitals.

Table I. *A*, *B*, and *C* Parameters (in eV), Deduced from Atomic Dirac–Slater Calculations[a]

				C		
atom	AO	*A*	*B*	*j**	*j*	av
Th	7s	−0.786	−3.00		−4.72	−4.72
	6p	−1.01	−3.72	−27.61	−20.01	−22.54
	6d	−0.874	−3.46	−3.12	−2.74	−2.89
	5f	−1.01	−3.66	−2.13	−1.56	−1.80
Pa	7s	−0.801	−3.07		−4.83	−4.83
	6p	−1.01	−3.84	−29.1	−20.8	−23.6
	6d	−0.887	−3.55	−3.15	−2.75	−2.91
	5f	−1.01	−3.80	−3.23	−2.52	−2.82
U	7s	−0.816	−3.13		−4.91	−4.91
	6p	−1.02	−3.93	−30.49	−21.48	−24.48
	6d	−0.906	−3.62	−3.15	−2.72	−2.89
	5f	−1.02	−3.89	−4.25	−3.41	−3.77
Np	7s	−0.836	−3.17		−5.01	−5.01
	6p	−1.04	−3.99	−31.8	−22.1	−25.33
	6d	−0.930	−3.66	−3.13	−2.69	−2.87
	5f	−1.04	−3.95	−5.22	−4.25	−4.67

[a] The separate *C* values and their weighted average are given for the two spin–orbit-split components, $j = l \pm {}^1/_2$, denoted j^* and j, respectively.

2. Method

2.1. Program Modification. In ref 4, we obtained the diagonal energy parameters from Dirac–Slater calculations on the free atom A, with various electron configurations, giving the matrices **A** and **B**:

$$h_{aa} = \epsilon_a^0 + \sum_{b\in A} \mathbf{A}_{ab}(\delta n_b)^2 + \sum_{b\in A} \mathbf{B}_{ab}(\delta n_b) \qquad (1)$$

with $\delta n_b = n_b - n_b^0$. This simulated the intraatomic electron–electron repulsion. Transition-state atomic calculations[15] were used, corresponding to philosophy 3. We now add to the program[2] the option of replacing (1) by

$$h_{aa} = C_a + A_a^A(\delta Q_A)^2 + B_a^A(\delta Q_A) \qquad (2)$$

where Q_A is the total Mulliken population of atom A. No Madelung corrections will be used with this option, following philosophy 2. The simple EHT total energy

$$E_T = \sum_i^{occ} \epsilon_i \qquad (3)$$

is used.

2.2. Energy Parameters. The orbital energies for the atoms Th–Am are shown in Figure 1. While the DF and DS trends are similar, the absolute heights are not. In particular, the DF 5f level lies below the 6d level, starting already with Th. Therefore, DF (or transition-state DS) parameters will not reproduce the metal hybridizations correctly, compared to the calculations in Table III.

Another alternative is to use the DS *orbital energies* for a number of atomic configurations, such as

$$f^{n-3}d^1s^2,\ f^{n-3}d^1s^1,\ f^{n-3}d^1s^0 \qquad (4)$$

for the systems A, A^+, and A^{2+}, respectively, to determine the coefficients A_a and B_a. Our results are given in Table I and included in the ITEREX

Table II. Converged Quasirelativistic h_{aa} Parameters for Th and U

	$-h_{aa}$					
atom	7s	6p	7p	6d	5f	ref
Th	5.39[a]	27.83[a]	5.39[a]	10.11[b]	9.64[b]	11
	5.39[a]	27.83[a]	5.39[a]	9.92[c]	9.42[c]	*e*
	5.39[a]	27.83[a]	5.39[a]	10.22[d]	9.75[d]	*e*
U	5.50	30.03	5.50	9.19[b]	10.62[b]	11
	5.50	30.03	5.50	9.15[c]	10.58[c]	*e*
	5.50	30.03	5.50	9.33[d]	10.77[d]	*e*
					10.7[f]	*e*

[a] Frozen. [b] Converged on $(cp)_2An(s\text{-}cis\text{-}C_4H_6)$.[11] [c] Converged directly on the metallocene, $M(COT)_2$, assuming M–C = 267 pm, C–C = 140 pm, and C–H = 109 pm and traditional Hoffmann parameters for C ($\alpha_{2s} = -21.40$, $\alpha_{2p} = -11.40$ eV, $\zeta_{2s} = \zeta_{2p} = 1.625$) and H ($\alpha_{1s} = -13.6$, $\zeta_{1s} = 1.3$). Other metal parameters were taken from ref 11. [d] Converged directly on $M(cp)_4$, assuming M–centroid = 255 pm, C–C = 142 pm, and C–H = 109 pm. [e] Present work. [f] Reproduces Rösch's f character for $U(COT)_2$.[5,6]

Table III. Valence MO Orbital Energies, ϵ (eV), Metal Characters, *N*, and Metal Atom Mulliken Charges, *Q*, for Metallocenes, $M(COT)_2$

metal	$-\epsilon(e_{2g})$	*N*(d)	$-\epsilon(e_{2u})$	*N*(f)	*Q*	method
Th	12.07	0.237	11.43	0.191	1.514	REX[a,b]
	12.07	0.235	11.36	0.222	1.504	REX[a,f]
	12.14	0.252	11.44	0.273		
	5.50	0.211	4.49	0.203		MS–Xα[a,c]
	6.61	0.201	5.88	0.141		P-HFS[d]
	6.69	0.176	5.90	0.106		
U	11.84	0.201	11.58	0.335	1.308	REX[a,b]
	11.86	0.202	11.48	0.311	1.345	REX[a,f]
	11.93	0.221	11.61	0.374		
	5.27	0.198	4.49	0.327		MS–Xα[a,c]
	6.61	0.173	5.96	0.244		P-HFS[d]
	6.69	0.149	6.04	0.201		
					0.98	PP[e]

[a] Same geometries as in Table II. [b] Same parameters as in Table II. [c] References 5 and 6. Split components shown separately. [d] Perturbative Hartree–Fock–Slater, ref 8. [e] Pseudopotential SCF.[9] [f] Iterated, "final" parameters (see section 3.1).

Table IV. Valence MO Orbital Energies (in eV) and Percent Metal Characters for $(cp)_4M$[a]

			metal character		
metal	MO	energy	5f	6d	7p
Th	a_2	11.96 (4.98)	15 (14)		
	e	12.03 (5.00)	16 (14)		
	b_2	12.43	1 (1)	7 (8)	4 (2)
	e	12.44	1 (1)	7 (8)	3 (2)
	b_1	12.78		14 (17)	
	a_1	12.78		14 (17)	
U	e	10.77 (3.47)	90 (86)	2 (3)	
	a_2	12.01 (5.03)	25 (23)		
	e	12.08 (5.05)	25 (23)		
	b_2	12.39 (5.74)	2 (1)	6 (8)	3 (2)
	e	12.40 (5.77)	3 (1)	6 (8)	3 (2)
	b_1	12.62 (6.26)		11 (17)	
	a_1	12.63 (6.28)		12 (17)	

[a] The MS–Xα results of Bursten et al.[7] are given in parentheses. The symmetry labels refer to a D_{2d} symmetry.

(15) Liberman, D. A.; Cromer, D. T.; Waber, J. T. *Comput. Phys. Commun.* **1971**, *2*, 107.

Table V. Single-ζ Radial Parameters and Noniterative Energy Parameters for 7s and 6p Shells[a]

element	AO	ζ	α/eV
Th	7s	1.834	−5.31
	6p*	3.816	−33.23
	6p	3.417	−25.01
	6p(av)	3.550	−27.75
Pa	7s	1.876	−5.41
	6p*	3.923	−34.93
	6p	3.501	−25.95
	6p(av)	3.642	−28.94
U	7s	1.914	−5.51
	6p*	4.032	−36.51
	6p	3.582	−26.76
	6p(av)	3.732	−30.01
Np	7s	1.948	−5.61
	6p*	4.135	−38.03
	6p	3.661	−27.48
	6p(av)	3.819	−31.00

[a] For 7p, the 7s parameters can be used. Here 6p* and 6p stand for $6p_{1/2}$ and $6p_{3/2}$, respectively.

Table VI. Double-ζ Radial Parameters and Noniterative Energy Parameters (eV) for 6d and 5f AOs[a]

atom	AO	C_1	ζ_1	C_2	ζ_2	energy	ζ(single)
Th	6d*	0.7580	2.530	0.4120	1.196	−10.276	1.974
	6d	0.7614	2.416	0.4053	1.148	−9.896	1.898
	6d QR	0.7600	2.462	0.4080	1.167	−10.048	1.929
	5f*	0.7683	4.534	0.4237	1.875	−9.617	3.358
	5f	0.7673	4.439	0.4293	1.814	−9.047	3.260
	5f QR	0.7677	4.480	0.4269	1.840	−9.291	3.302
Pa	6d*	0.7605	2.593	0.4110	1.218	−10.004	2.023
	6d	0.7613	2.479	0.4080	1.170	−9.604	1.941
	6d QR	0.7611	2.525	0.4093	1.189	−9.764	1.974
	5f*	0.7771	4.774	0.4036	2.018	−10.330	3.625
	5f	0.7748	4.684	0.4106	1.960	−9.620	3.524
	5f QR	0.7758	4.723	0.4076	1.985	−9.924	3.567
U	6d*	0.7597	2.656	0.4148	1.240	−9.619	2.062
	6d	0.7592	2.537	0.4133	1.190	−9.194	1.975
	6d QR	0.7594	2.585	0.4139	1.210	−9.364	2.010
	5f*	0.7858	4.996	0.3866	2.142	−10.863	3.866
	5f	0.7825	4.906	0.3945	2.084	−10.021	3.761
	5f QR	0.7839	4.945	0.3911	2.109	−10.382	3.806
Np	6d*	0.7552	2.718	0.4231	1.261	−9.422	2.093
	6d	0.7551	2.590	0.4212	1.208	−8.982	2.000
	6d QR	0.7551	2.641	0.4219	1.229	−9.158	2.037
	5f*	0.7941	5.198	0.3725	2.246	−11.142	4.080
	5f	0.7903	5.104	0.3809	2.186	−10.172	3.969
	5f QR	0.7919	5.144	0.3773	2.212	−10.588	4.017

[a] These energies are the converged ones for the actinocenes, see section 3.1. The last column gives a single-ζ fit to the DZ orbital.

program.[2] When iterated to self-consistency on $(cp)_2An(s\text{-}cis\text{-}C_4H_6)$ the h_{aa} parameters assume the values given in Table II. Iterations on other systems, such as $An(cp)_4$ or $An(COT)_2$ give closely similar values (see Table II). We note that the metal characters (Tables III and IV) now are comparable to the MS-Xα or P-HFS ones. To obtain these metal characters, we require that $h_{6d} < h_{5f}$ and $h_{5f} < h_{6d}$ for Th and U, respectively. Closely similar values for the 6d and 5f h_{aa} parameters are obtained by simply requiring that they reproduce the MS-Xα populations. Obviously, a reservation must be made for comparing populations, N, for different basis sets in Table III. Summarizing, for the 6d and 5f orbitals, we recommend iterations with the parameters in Table I. For noniterative calculations on organometallic systems, the parameters in Table VI may be used.

The 7s energies depend only weakly on Z while the 6p energies decrease rapidly with Z (Figure 1). The $s^2d^1f^n$ DF 7s and 6p orbital energies[14,16] (reproduced in Table V) can be chosen for noniterative calculations. If iterations are required, the ones in Table I may be used. For simplicity, the 7p orbitals can be given the same parameters as the 7s orbital.

2.3. Radial Parameters. Single-ζ (SZ) parameters for all actinoids from DF calculations for neutral atoms are given in ref 1 and, as defaults, in the REX programs. Double-ζ (DZ) (DF, $s^2d^1f^n$) fits for Th–Am also exist.[14] DZ fits to Desclaux's[16] $\langle r^n \rangle$ were used by one of us in all earlier work for the 6d and 5f orbitals of Th and U.[10-12]

The SZ 6p and 7s (=7p) parameters in Table V are r_{max} ones for the $7s^26d^15f^n$ configurations, $\zeta = n/r_{max}$, where r_{max} is the radius for maximum electron density. Note that the 6p ζ values used earlier by one of us[10-12] were the 6p* ones.

The uranium 6d and 5f orbitals from direct fits to radial densities and from fits to $\langle r \rangle$, $\langle r^2 \rangle$, and r_{max} are found to be rather similar. The latter ones and their weighted, quasirelativistic averages are shown in Table VI.

As to the trends among radial functions along the series Th–Am, the 6d radial functions contract only slightly from Th to Am, while the 5f ones contract a great deal.

(16) Desclaux, J. P. *At. Data Nucl. Data Tables* **1973**, *12*, 311.

Table VII. Ratios of the 5f and 5f* Mulliken Populations in the $3e_{2u}$ δ-Bonding MO of the Actinocenes[a]

	$N(5f)/N(5f^*)$			
method	Th	Pa	U	Np
P-HFS[8]		0.96	0.82	0.69
ITEREX	0.81	0.68	0.42	0.22

[a] The REX calculations use the standard geometry in Table II. The HFS calculations use the calculated, relativistic An–C. The statistical, nonrelativistic limit of $N(f)/N(f^*)$ is 8/6 = 1.333.

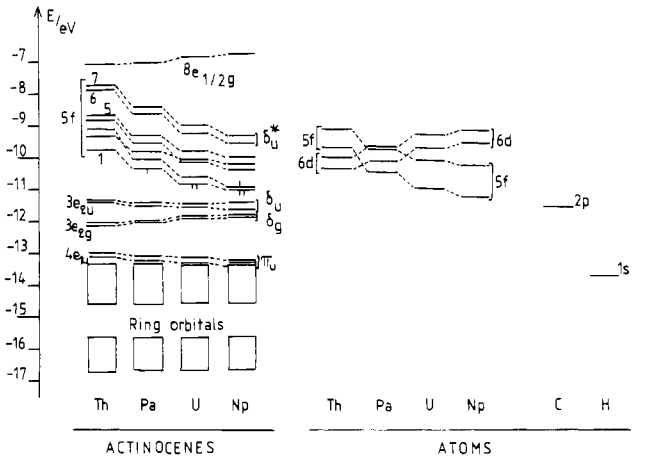

Figure 2. Orbital energies from the present, iterative REX calculation for the actinocenes $An(COT)_2$, An = Th–Np. Labels 1–7 for the 5f levels stand for $6e_{5/2u}$, $5e_{7/2u}$, $9e_{1/2u}$, $8e_{3/2u}$, $10e_{1/2u}$, $9e_{3/2u}$, and $7e_{5/2u}$, respectively, in the notation of Boerrigter et al.[8]

3. Results

3.1. Actinocenes. As a final test on the present parameters, we reran the actinocenes (An = Th–Np) at the standard geometry in Table II using the spin–orbit-split parameters.

Apart from Boerrigter's work, ours is the only one including spin–orbit effects. An interesting question is whether or not they influence the bonding and reactions of actinoid organometallics. A transition from 5f bonding toward "5f* ($5f_{5/2}$) bonding" in the $3e_{2u}$ δ bonding orbital is clearly seen in Table VII. In the REX case this trend is stronger than in the P-HFS case. What, if any, its chemical consequences would be is still an open question. The corresponding ratio for the total 5f character of all occupied levels of thorocene is 0.83, as compared to 0.81 for the $3e_{2u}$ MO in Table VII.

The frozen 7s, 6p, and 7p parameters in Table V are used, together with the 6d and 5f iteration parameters in Table I and the DZ radials in Table VI. Because the spin–orbit splitting would increase the total 5f character from its quasirelativistic value, due to the predominance of 5f* over 5f bonding, the C constants of the 5f* and 5f levels were actually shifted upward by the 5f(QR) − 5f* difference in the actinocene calculation.

The converged 6d and 5f orbital energies, h_{aa}, for the actinocenes are shown in Table VI and the molecular energy levels in Figure 2. This figure is very similar to Boerrigter's[8] one for the highest three metal-to-ring bonding orbitals ($4e_{1u}$, $3e_{2g}$, and $3e_{2u}$) and also for the seven, mainly 5f ones, above them, if our levels are shifted upward by some 5–6 eV. Our lowest 6d level lies higher than his. The 6d LUMO of thorocene[8] is probably real; the ground state[17]

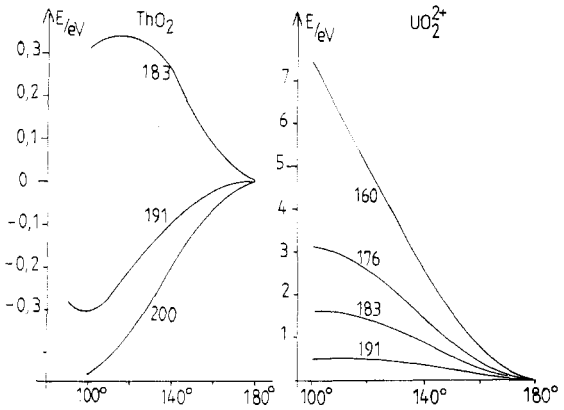

Figure 3. REX total energies for ThO_2 and UO_2^{2+} at different bond lengths.

of Th(III) in $Th[\eta^5\text{-}C_5H_3(SiMe_3)_2]_3$ is $6d^1$, not $5f^1$.

Our 5f levels have approximately the same order as Boerrigter's.[8] The total 5f bandwidths are also comparable. Particularly noteworthy are the antibonding $5f\delta_u^*$ levels 6 and 7, which could be called an antibonding "mirror image" of the δ_u bonding orbital, indicating also the involvement of the 5f AOs in bonding.

For the $4e_{1u}\pi_u$ bonding MO, our 6p-induced relativistic splittings vary from 0.13 to 0.10 eV for Th–Np, compared to Boerrigter's value of about 0.21 eV. Our final metal characters in the two δ-bonding MOs ($3e_{2g}$ and $3e_{2u}$) are close to the QR ones in Table III and also given there.

An obvious point is that we here give one-electron energy levels. If transition energies or magnetic moments of f^n systems for $n > 1$ are desired, the intra-5f interactions are essential, as discussed, e.g., in ref 8.

3.2. Geometries of UO_2^{2+} and ThO_2. The solid-state geometry of uranyl is closely linear,[18] with U–O varying from ca. 160 ("150 (3)") to over 190 pm. On the contrary, molecular-beam deflection[19] of ThO_2 shows a permanent dipole moment and matrix-isolation IR spectra of ThO_2 in Ar suggest an O–Th–O angle of 122.5 (2)°.[20] The isovalent d-electron systems VO_2^+, MoO_2^{2+}, and WO_2^{2+} also are strongly bent (O–M–O = 102–114°).[12]

The reasons are intriguing. Uranyl differs from its d-electron analogues by having available 5f orbitals and also by having a chemically accessible, "semicore" 6p shell. Tatsumi and Hoffmann[12] suggested that these "cooperate", leading to a "6p activation" of the 5f orbitals. Replacing the 6p–2p antibonding character in the σ_u HOMO by 5f–2p bonding allows one also to understand the short U–O bond length.[4] While the strong, multiple bonds of the actinyls involve the 6d and 5f orbitals, the particular MO keeping uranyl linear in an EHT[21] (or REX[1,4,14]) picture is the penultimate occupied one (no. 10). Pyykkö and Laaksonen[14] suggested that the raising of MO 10 upon bending would actually come from the $2p(O)\text{–}6p_{3/2}(U)$ antibonding orbital and would not involve the 5f orbitals. Without the 5f orbitals, the HOMO (MO 11) would tend to bend the system, however.[4]

Concerning the difference between thorium and uranium, Wadt[13] aptly remarked that the 6p orbitals are present in Th as well. He explained the different geometries of ThO_2 and uranyl by their different metal hybridizations ($d^{1.19}f^{1.06}$ and $d^{1.20}f^{2.41}$ at 180° for Th and U, at R = 192 and 164 pm, respectively). He obtained a linear uranyl for his effective core potential Hartree–Fock method, whether the An 6p shell was in the valence space or in the core, questioning the need for 6p:s to hold uranyl linear.

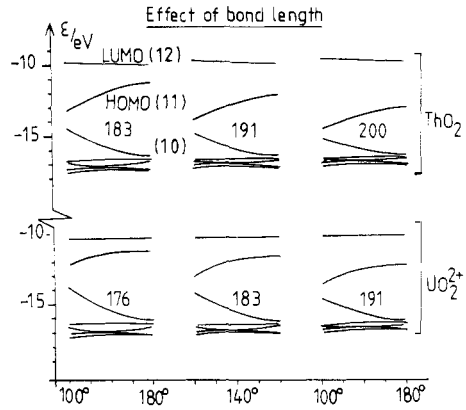

Figure 4. Effect of bond length on the Walsh diagrams of ThO_2 and UO_2^{2+}.

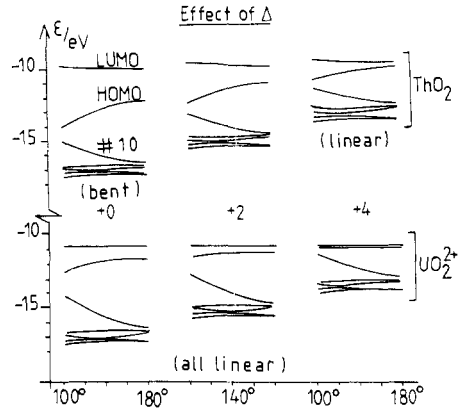

Figure 5. Effect of shifting the oxygen energy levels upward for a typical bond length.

Table VIII. Orbital Energy Differences ($\epsilon(100) - \epsilon(180)$, in eV) for ThO_2 and UO_2^{2+} at $\Delta = 0^a$

		orbital energy diff			
molecular	MO	M–O = 176 pm	M–O = 183 pm	M–O = 191 pm	M–O = 200 pm
ThO_2	11		−1.9	−1.8	−1.4
	10		+2.1	+1.6	+1.2
	sum		+0.2	−0.2	−0.2
UO_2^{2+}	11	−1.0	−1.3	−1.3	
	10	+2.4	+2.0	+1.5	
	sum	+1.4	+0.7	+0.2	

[a] A positive sum indicates a linear molecule.

Describing Th as rather more a "d metal" and U as an "f metal" was our central concern in the present work. Besides this difference of the elements, the bond lengths are different. Wadt calculated a Th–O distance of 191 pm, rather longer than most U–O distances.

We now have bent both ThO_2 and uranyl as a function of the bond length. The default oxygen parameters in the program[1] were used, eventually shifting these energies upwards by Δ = 0, +2 or +4 eV to avoid excessive ionicity, as in ref 1. The QR parameters of ref 11 were used for Th and U, except for the 6p orbitals where the effects of spin–orbit splitting were introduced[16] (and found to be small). Bond lengths of 183, 191, and 200 pm and 176, 183, and 191 pm were used for the two systems, respectively.

For a metal described by the U parameters, the system is clearly linear for every distance, and more strongly so for the shorter ones. With the Th parameters (note the scale difference) the system is linear at R = 183 pm and bent at R = 191 and 200 pm (see Figure 3). Here the oxygen shift, Δ, is set equal to zero.

Thus the properties of the metal clearly count. Asking why, we look at the orbital energy diagrams. Figure 4 shows the Walsh diagrams for different bond lengths. Figure 5 shows the depen-

(17) Kot, W. K.; Shalimoff, G. V.; Edelstein, N. M.; Edelman, M. Lappert, M. F. *J. Am. Chem. Soc.* **1988**, *110*, 986.
(18) *Gmelin Handbook of Inorganic Chemistry*; Springer Verlag: West Berlin, 1983; *U Supplement A6*.
(19) Kaufman, M.; Muenter, J.; Klemperer, W. *J. Chem. Phys.* **1967**, *47*, 3365.
(20) Gabelnick, S. D.; Reedy, G. T.; Chasanov, M. G. *J. Chem. Phys.* **1974**, *60*, 1167.
(21) Unpublished details of ref 12.

dence on Δ (an upward shift of the oxygen 2p orbitals). It is seen that the HOMO energy becomes almost independent of angle, if it becomes too close to the empty 5f-like levels. (The sum of the five lowest orbital energies is approximately independent of the angle and is therefore omitted from Figures 4 and 5.) The central feature for Th, as a function of decreasing bond length, is seen to be that the "linearizing" influence of MO 10 grows faster than the bending influence of MO 11, with shortening bond length. This tendency is seen quantitatively in Table VIII.

Comparing the two metals, the linearizing tendency of MO 10 and the R dependence of this trend are very similar. The difference appears in MO 11 where the bending tendency is stronger for Th than for U.

A variation of Δ for ThO_2 at 191 pm gives a bent molecule for Δ = 0, two minima (at 180 and 100°) for Δ = 2 and a clearly linear molecule at 4 eV. For uranyl, all Δ values give a linear molecule (see Figure 5).

Without the 6p orbitals, using a 7s7p6d5f metal basis, all cases were linear but only very weakly.

The Walsh-type REX argument, based on the energies of MOs 10 and 11, can be summarized as follows (the bond lengths are here input data).

ThO_2 is bent, first because it has a larger bond length and therefore a weaker "linearizing" tendency from MO 10 (see Figure 4), second because it has lower lying 6d levels (in ref 11 as in Figure 2 but not in Figure 1) that tend to bend the molecule and, third because it has a higher lying 5f level, which therefore does not "flatten" the HOMO, MO 11.

Inversely, uranyl is linear because it has a shorter bond length (due to good multiple bonding, a smaller 6p core and, eventually, its positive net charge) and has therefore a strong linearizing tendency from the MO 10, second uranium has higher lying input 6d levels, and third uranium has lower lying input 5f levels, which tend to "flatten" MO 11.

To obtain the strong 5f character of MO 11 the REX/EHT requires the "pushing from below" by the semicore 6p AOs. With the 6p but without the 5f orbitals, MO 11 would be strongly bending.[4,12] Without the 6p orbitals, MO 10 would not become strongly linearizing because this trend was attributed to 2p–6p repulsion.[14]

As a technical detail, it is interesting that the σ_u MO 11 is apparently repelled by the 5f band above it, although none of the other 5f levels have a σ_u symmetry that could lead to a noncrossing. Similar stationary levels have been reported elsewhere[22-24] for Hamiltonian matrices of the type

$$\mathbf{h} = \begin{pmatrix} \alpha_1 & 0 & a \\ 0 & \alpha_1 & b \\ a & b & \alpha_3 \end{pmatrix} \tag{5}$$

In that case the combination $b|1\rangle - a|2\rangle$ of the two degenerate orbitals is orthogonal to $|3\rangle$ and stays at $E = \alpha_1$.

In the present case, we instead have the matrix structure

$$\mathbf{h} = \begin{pmatrix} \alpha_{6p} & 0 & a \\ 0 & \alpha_{5f} & b \\ a & b & \alpha_{2p} \end{pmatrix} \tag{6}$$

This matrix has an (Newton–Raphson, $\mathbf{S} = \mathbf{1}$, $\alpha_{5f} = 0$) eigenvalue at

$$E \cong \alpha_{6p} b^2/(a^2 + b^2 - \alpha_{6p}\alpha_{2p}) \tag{7}$$

As, typically, $a = +17$ eV, $b = +3$ eV, $\alpha_{6p} = -19$ eV, $\alpha_{2p} = -6$ eV for Δ = 0, this level lies about 1 eV below α_{5f}.

Acknowledgment. We thank Jukka Tulkki for some atomic DF calculations, Evert Jan Baerends and Jaap Snijders for helpful comments, and a reviewer for asking that the last point be clarified.

Registry No. UO_2^{2+}, 16637-16-4; ThO_2, 1314-20-1; $(cp)_4Th$, 1298-75-5; $(cp)_4U$, 1298-76-6; $Th(COT)_2$, 12702-09-9; $U(COT)_2$, 11079-26-8; $Pa(COT)_2$, 51056-18-9; $Np(COT)_2$, 37281-22-4.

(22) Burdett, J. K. *Prog. Solid State Chem.* **1984**, *15*, 173, 241.
(23) Hoffmann, R.; Li, J.; Wheeler, R. A. *J. Am. Chem. Soc.* **1987**, *109*, 6600.
(24) Boerrigter, P. M.; Snijders, J. G.; Dyke, J. M. *J. Electron Spectrosc. Relat. Phenom.* **1988**, *46*, 43.

Contribution from the Department of Chemistry, University of Leuven, Celestijnenlaan 200F, 3030 Heverlee, Belgium

Electronic Configuration and Orbital Energies: The 3d–4s Problem

L. G. Vanquickenborne,* K. Pierloot, and D. Devoghel

Received May 6, 1988

With the use of the numerical Hartree–Fock method, a set of average-of-configuration calculations have been carried out for the atoms from H to Cu, as well as for the corresponding mono- and dipositive ions. The focus of this work is on the study of the occupation of 3d and/or 4s orbitals. Attempts are made to relate configurational energy differences to simple orbital energy differences, so as to provide additional insight into the Aufbau principle of the periodic system of the elements.

I. Introduction

In discussions of the Aufbau principle of the elements, it is customary to start from a qualitative energy diagram,[1-3] where the evolution of the different orbital energies ε is shown as a function of Z. Up to argon, the ground-state configuration of the atoms can be obtained by filling the orbitals in the expected sequence 1s, 2s, 2p, 3s, 3p. The first deviation from the hydrogenic order is apparently due to a crossover of the 3d and 4s curves. Obviously, the 3d–4s crossover has important consequences for the electronic configuration of transition-metal elements.

Yet, it appears that the theoretical basis of the $\epsilon(Z)$ orbital energy diagram is somewhat unclear: the diagrams presented in the literature either are purely qualitative, are deduced from spectral data in a semiempirical way, or else are based on very approximate Thomas–Fermi-type calculations. To our knowledge, no systematic ab initio treatment is available, describing the evolution of the orbital energies ε as a function of Z.

It is the purpose of this paper (i) to discuss a systematic series of ab initio calculations on the relevant configurations with 4s and/or 3d occupation, from H up to Cu, (ii) to relate configurational energy differences to orbital energy differences, and (iii) to extend the calculations to the mono- and dipositive ions of the elements.

II. Hartree–Fock Treatment of the Average of a Configuration

For the systems under consideration, it is possible to predict the experimental ground states and to calculate quantitatively term splittings and ionization energies by MCSCF type techniques and configuration interaction.[4-7] If one is more interested in general

(1) Latter, R. *Phys. Rev.* **1955**, *99*, 510.
(2) Levine, I. N. *Quantum Chemistry*; Allyn & Bacon, Inc.: Boston, MA, 1974; p 244.
(3) Cotton, F. A.; Wilkinson, G. *Advanced Inorganic Chemistry*, 5th ed.; J. Wiley & Sons, Inc.: New York, 1988; p 628.

0020-1669/89/1328-1805$01.50/0